Korean J. Chem. Eng., 32(7), 1434-1439 (2015)
DOI: 10.1007/s11814-014-0313-y

pISSN: 0256-1115
eISSN: 1975-7220

Influence of crosslinker amount on swelling and gel properties of hectorite/poly(acrylamide/itaconic acid) nanocomposite hydrogels

Tao Wan*,,†, Wenzhong Cheng*, Zhiling Zhou*,†, Min Xu*, Chuzhang Zou*, and Ruixiang Li***

*Mineral Resources Chemistry Key Laboratory of Sichuan Higher Education Institutions, Chengdu University of Technology, Chengdu 610059, Sichuan, China
**State Key Lab of Geohazard Prevention & Geoenvironment Protection, Chengdu University of Technology, Chengdu 610059, Sichuan, China
(*Received 26 June 2014 • accepted 20 October 2014*)

Abstract−A new hectorite/poly(acrylamide/itaconic acid) nanocomposite hydrogel was synthesized by inverse microemulsion polymerization. The effects of crosslinker amount on water absorbency and salt absorbency, swellability, pH-sensitivity, gel strength, temperature-and shear-resistance were investigated. Water and salt absorbencies, pH-sensitivity and swellability decreased, while gel strength and temperature-and shear-resistance increased with increasing crosslinker amount. Nanocomposite hydrogels had good thermal stability with onset decomposing temperature of 252 °C. The as-synthesized hydrogel particles were regular and spherical-like and had an average particle size of 43 nm in the range of 30-65 nm. Hectorite clay platelets were exfoliated and transformed into amorphous structure.

Keywords: Hydrogel, Nanocomposite, Hectorite, Microemulsion Polymerization

INTRODUCTION

Superabsorbent hydrogels have been widely applied in many fields as hygienic products [1], in agriculture [2], waste water treatment [3], drug-delivery systems [4] and enhanced oil recovery [5]. However, superabsorbent hydrogels made from either natural or synthetic sources are limited in their industrial and biomedical applications due to their poor mechanical properties caused by irregularly distributed crosslinking. Many efforts have been focused toward enhancing the mechanical strength of these hydrogels [6,7]. Nanocomposite hydrogels (NC gels), having complex nanometer-scale structures, exhibit extraordinary mechanical and optical properties and could overcome the limitations of conventional chemically crosslinked hydrogels [8-13].

Laponite, ($Na^{+}_{0.7}[(Mg_{5.5}Li_{0.3})Si_8O_{20}(OH)4]^{-0.7}$), consists of synthetic silicate nanoparticles with an average diameter of 30 nm and a thickness of 1 nm. Contrary to the conventional chemically crosslinked hydrogels, the NC gels formed using Laponite as a multifunctional crosslinker exhibit extraordinary mechanical toughness, tensile moduli, and tensile strengths [14-19]. But, the expensive price of Laponite is disadvantageous to applications in industrial production on a large scale.

Up to now almost all of the Laponite-based NCs have been prepared by water solution polymerization. Little is reported about the acrylamide-itaconic acid/clay nanocomposite hydrogel. Kiatkamjornwong [20] synthesized acrylamide-itaconic acid/mica hydrogel nanocomposites by water solution polymerization, using ammonium persulfate and N, N, N′, N′-tetramethylethylenediamine as the redox initiators and mica as an inorganic additive. Water absorbency and the artificial urine absorbency of the nanocomposite with an AM/IA mole ratio of 95 : 5, 0.2% mol MBA, and 5% w/w mica were 748 g/g and 76 g/g, respectively. The viscoelastic behavior suggested that the swollen gel of the nanocomposites exhibited mechanical stability and elasticity. Kaplan [21] prepared acrylamide-itaconic acid/montmorillonite (MMT) hydrogel nanocomposites by water solution polymerization, using polyethyleneglycol (400) diacrylate as crosslinker. The hydrogel nanocomposite has high adsorption rate (equilibrium time is approximately 30 min) and basic dye adsorption capacity of 458.1 mg/g.

On the base of our previous work on superabsorbent hydrogels and microemulsion polymerization [22-32], a novel hectorite/poly (acrylamide/itaconic acid) nanocomposite hydrogel was synthesized by inverse microemulsion polymerization, using a commercial synthesized and cheap hectorite product as replacer of Laponite. The hectorite clay is dispersed in aqueous monomer solutions and then added into the inverse microemulsion. Finally, the nanocomposite hydrogel latex with nanoscale particle size is prepared by inverse microemulsion polymerization. Effects of crosslinker amount on water absorbency and salt absorbency, swellability, gel strength, temperature-and shear-resistance were investigated. Structures and thermostability of the nanocomposite hydrogels were characterized by transmission electron microscope (TEM), X-ray diffraction (XRD) and thermal gravimetric analysis (TGA), respectively. These nanocomposite hydrogels showed good pH-sensitivity, swellability, gel strength and temperature-and-shear-resistance, depending on the crosslinker amount.

†To whom correspondence should be addressed.
E-mail: wantaos@126.com, 34913755@qq.com

EXPERIMENTAL

1. Materials

Itaconic acid (IA), analytical grade, was purified by recrystallization. Acrylamide (AM), analytical grade, was purified by recrystallization. N-methylene-bis-acrylamide (MBA), analytical grade, was purified by recrystallization. Ammonium persulfate (APS), sodium bisulfite (SBS), sorbitan monooleate (Span-80), polyoxyethylene sorbitan monooleate (Tween 80), cyclohexane, analytical grade, were used without further purification.

2. Synthesis of Hectorite/Poly(Acrylamide/Itaconic Acid) Nanocomposite Hydrogels

A series of nanocomposite hydrogels with different components were prepared by microemulsion polymerization according to the following procedure: Typically, 0.45 g hectorite was dispersed in 30 mL distilled water under stirring at least for 4 h to make a uniform dispersion. Then 2.25 g itaconic acid and desired amounts of NaOH solution were added into the hectorite aqueous dispersion in an ice bath. Subsequently, 9 g acrylamide and 0.034 g N-methylene-bis-acrylamide were added to the above aqueous dispersion under stirring at room temperature for 60 min. Finally, the mixed aqueous dispersion was added dropwise to the inverse microemulsions formed by 300 g cyclohexane, 18 g Span80, and 12 g Tween 80. The water bath was heated slowly to 45-55 °C with mild stirring under bubbling N_2 gas after redox initiator APS (69 mg) and sodium bisulfite (19 mg) were introduced to the above inverse microemulsions. After 3-5 h of the reaction, the resulting product was washed several times with ethanol and acetone, respectively, dried at 60 °C to a constant weight, and then milled and screened.

3. Water Absorbency of the Nanocomposite Hydrogels Using Filtration Method

Approximately 50 mg of dried, milled and sifted hydrogels was dispersed in 100 mL of deionized water. Then, excess water was allowed to drain through a 300 mesh wire gauze. The weight of the hydrogels containing absorbed water was measured, and water absorbency at different absorption time was calculated according to the following equation:

$$\text{Water absorbency (g/g)} = (W_2 - W_1)/W_1 \quad (1)$$

where W_1 and W_2 are the weight of the dry and swollen hydrogels, respectively.

4. Saline Solution Absorbency of the Nanocomposite Hydrogels Using Filtration Method

Approximately 20 mg of dried, milled and sifted hydrogels was dispersed in 50 mL 1%, 3%, 5%, 10%, 15% NaCl, $MgCl_2$ and $CaCl_2$ solutions for 300 min, respectively. Then, excess salt solutions were allowed to drain through a 300 mesh wire gauze. The weight of the hydrogels containing absorbed salt solutions was measured after draining for 30 min, and the saline solution absorbency was calculated according to the following equation:

$$\text{Saline solution absorbency (g/g)} = (S_2 - S_1)/S_1 \quad (2)$$

where S_1 and S_2 are the weight of the dry and swollen hydrogels, respectively.

5. Determination of Swellability of the Nanocomposite Hydrogels

Particle sizes of the nanocomposite hydrogels swollen at different time were determined by an OMEC LS-POP(III) laser particle size analyzer (Zhuhai OMEC instrument Co., Ltd., China).

6. Gel Properties of the Nanocomposite Hydrogels Determined by Rotation Viscometer

6-1. Gel Strength Evaluation of the Nanocomposite Hydrogels

Approximately 50 mg of dried, milled and sifted hydrogels was dispersed in 100 mL of deionized water. After reaching water absorption equilibrium, excess water was allowed to drain through a 300 mesh wire gauze. Gel strength of the water-swollen nanocomposite hydrogels could be measured by apparent viscosity and was determined on a NXS-11B type rotation viscometer (Chengdu, China) at a shear rate of 17 s-1 at room temperature.

6-2. Shear-resistance Evaluation of the Nanocomposite Hydrogels

Swollen nanocomposite hydrogels were agitated by a high-speed mixer for 60 min with a speed of 3,000 rpm, and then the gel strength of the swollen nanocomposite hydrogels was determined on an NXS-11B type rotation viscometer (Chengdu, China) at a shear rate of 17 s-1 at room temperature.

6-3. Temperature-resistance Evaluation of the Nanocomposite Hydrogels

Swollen nanocomposite hydrogels were placed in an oven at 80 °C, taken away every 1 h, cooled to room temperature and then the gel strength of the swollen nanocomposite hydrogels was determined on an NXS-11B type rotation viscometer (Chengdu, China) at a shear rate of 17 s-1.

7. Characterization of the Nanocomposite Hydrogels

The micrographs of nanocomposite hydrogels were taken using TEM (Tecnai G2 F20S-TWIN, FEI). Before TEM observation, inverse microemulsion samples were diluted with cyclohexane, stained with phosphotungstic acid, and then dipped onto the copper grid and allowed to evaporate at room temperature. X-ray diffraction measurements were performed using an X-ray diffractometer, Bruker AXS Model D8 Discover (Cu Kα radiation, 40 kV, 40 mA, with λ=0.15406 nm and n=1) at a scanning range from 10 to 60° and a scanning rate of 0.0258 min-1. TGA was recorded on a Dupont 2100 thermogravimetric analyzer, in the temperature range of 25 to 500 °C at a heating rate of 10 °C/min using dry nitrogen purge at a flow rate of 30 mL/min.

RESULTS AND DISCUSSION

1. Effect of Crosslinker Amount on Water Absorbency of the Nanocomposite Hydrogels

Crosslinking density plays a major role in modifying the swelling properties of hydrogels. Effects of crosslinker amount on the water absorbency of the nanocomposite hydrogels are shown in Fig. 1. Water absorbency decreased with increasing crosslinker amount.

The relationship between the volume swelling ratio $Q^{5/3}$ and network structure parameters given by Flory-Rehner theory [33] is usually used as the following equation:

$$Q^{5/3} = \left[\left(\frac{i}{2V_u I^{1/2}}\right)^2 + \frac{1/2 - \chi_1}{V_1}\right] / v_e/V_0 \quad (3)$$

Here, i/V_u is the concentration of the fixed charges referred to the unswollen polymer, and I is ionic strength in the external solution; the term $(1/2-\chi_1)/V_1$ represents the interaction parameter,

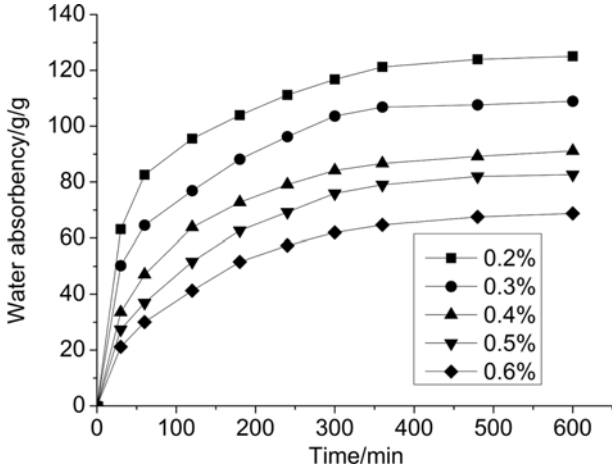

Fig. 1. Effect of crosslinker amount on water absorbency of the nanocomposite hydrogels.

i.e., affinity of the gel to water, and v_e/V_0 is the crosslink density of the gel.

According to Eq. (3), the volume swelling ratio $Q^{5/3}$ should increase as the square of concentration of the fixed charge and as the reciprocal of I, and decrease as the crosslink density. Higher crosslinker amount will result in more crosslink points and higher crosslink density, decreasing both the space among the grids of the three-dimensional network and the elasticity of the polymeric network. This will make it more difficult for the network to expand and be swollen by water, and therefore decrease water absorbency of the nanocomposite hydrogels. The results are in conformity with Flory-Rehner theory [33].

2. Effects of Crosslinker Amount on Salt Absorbencies of the Nanocomposite Hydrogels

Crosslinker amount dependence of salt absorbencies of the nanocomposite hydrogels was investigated and the results are in Fig. 2. Salt solution absorbencies decreased with increasing crosslinker amount. It is observed that, the lower the salt concentration, the higher the cation valence, the less the radius of the same valance cation, the more the salt solution absorbencies ($Na^+ > Mg^{2+} > Ca^{2+}$). According to the Donnan equilibrium theory, the distribution in the concentration of mobile ions between the gel and solution is reduced with increasing ionic strength, consequently decreasing the osmotic swelling pressure of the mobile ions inside the gel and decreasing salt solution absorbencies. Besides, with increase in ion size, salt solution absorbencies decrease due to the difficulty in the penetration of the ions into the hydrogel networks [34].

3. Effects of Crosslinker Amount on the pH-sensitivity of the Nanocomposite Hydrogels

Effects of crosslinker amount on the pH-sensitivity of the nanocomposite hydrogels are shown in Fig. 3. As indicated in Fig. 3, the swelling capacity of the nanocomposite hydrogels increased with increasing pH value until reaching the maximum, and then decreased with increasing pH value. Note that the pH-sensitivity decreased, whereas the maximum swelling capacity of the nanocomposite hydrogels occurred at higher pH value with increased crosslinker amount. Higher crosslinker amount can make the polymeric

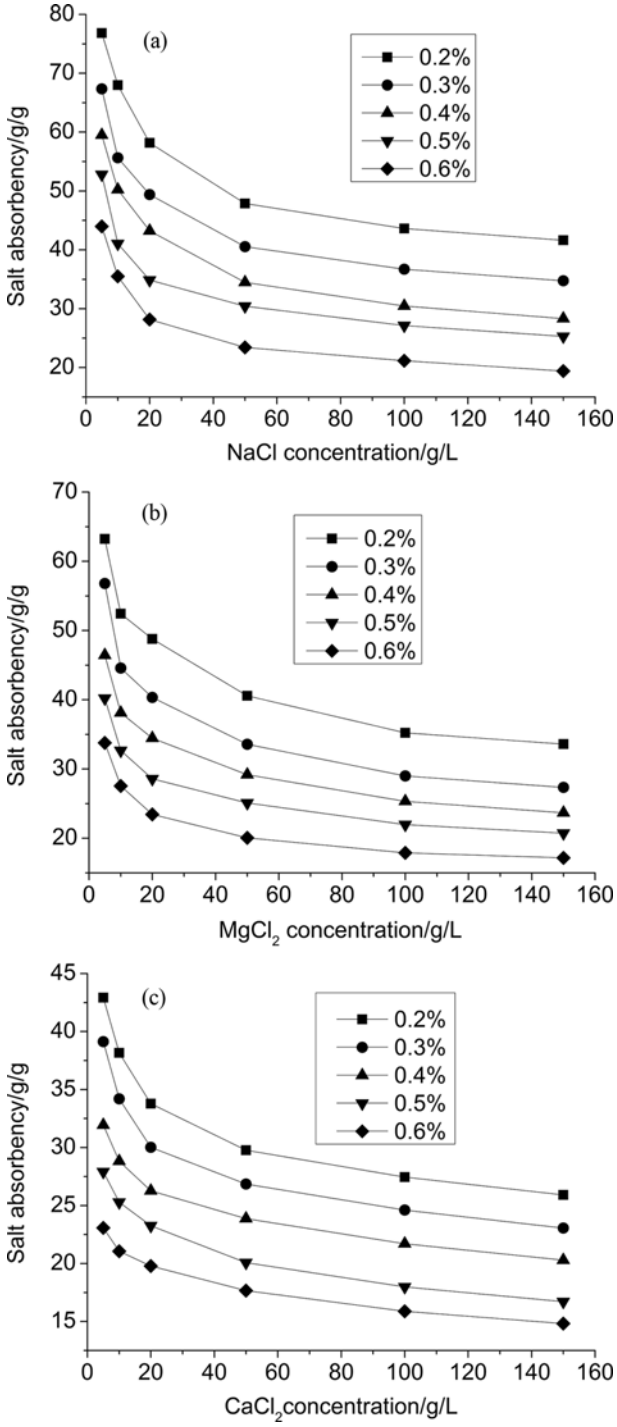

Fig. 2. Effects of crosslinker amount on salt absorbencies of the nanocomposite hydrogels.

chains more rigid and restrain the expansion of polymeric networks, thus decreasing pH-sensitivity of the nanocomposite hydrogels. Loose and flexible network can be formed under low crosslinker amount. This can make H^+ or OH^- enter into the network easily, and affect the ionization or deionization of carboxylate groups as well as the ionic strength of the hydrogels. Consequently, swelling capacity changes significantly and the maximum swelling occurs

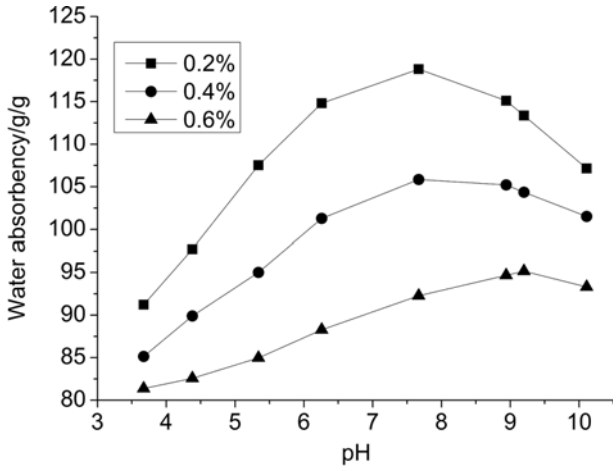

Fig. 3. Effects of crosslinker amount on the pH-sensitivity of the nanocomposite hydrogels.

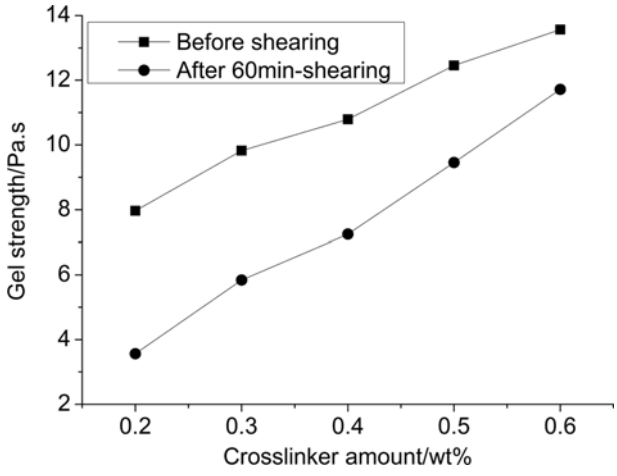

Fig. 4. Effects of crosslinker amount on the gel strength and shear-resistance of the nanocomposite hydrogels.

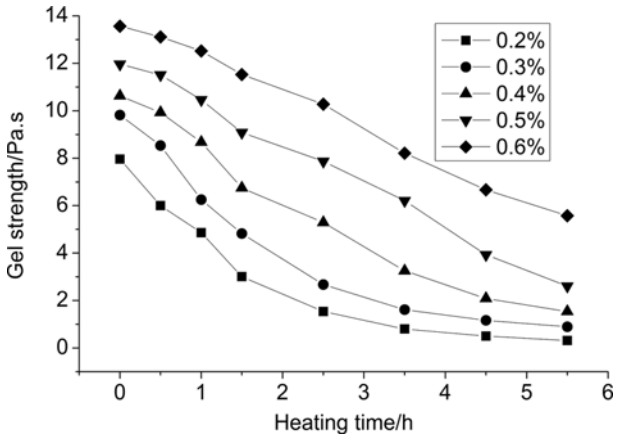

Fig. 5. Effects of crosslinker amount on temperature-resistance of the nanocomposite hydrogels.

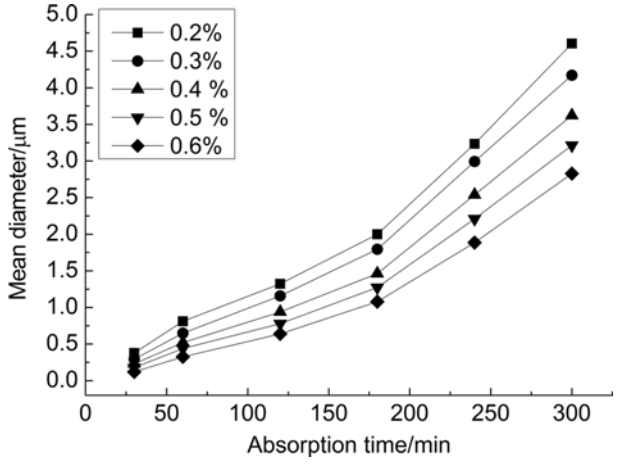

Fig. 6. Effects of crosslinker amount on swellability of the nanocomposite hydrogels.

at lower pH value with decreasing crosslinker amount.

4. Effects of Crosslinker Amount on the Gel Strength and Shear-resistance of the Nanocomposite Hydrogels

Fig. 4 demonstrates the gel strength and shear-resistance versus crosslinker amount of the nanocomposite hydrogels. Gel strength increased with increasing crosslinker amount and reached 13.6 Pa·s at 0.6 wt% crosslinker used. After 60 min-shearing with a speed of 3,000 rpm, gel strength of the nanocomposite hydrogels decreased, showing shear-thinning behaviors. However, gel strength of the nanocomposite hydrogels decreased more slightly after 60 min-shearing with increasing crosslinker amount, demonstrating enhanced shear-resistance of the nanocomposite hydrogels. Higher crosslinker amount can increase the effective network chain density of the nanocomposite hydrogels. This can make the polymeric chains more rigid and restrain the deformation of polymeric chains, thus increasing both gel strength and shear-resistance of the nanocomposite hydrogels.

5. Effects of Crosslinker Amount on Temperature-resistance of the Nanocomposite Hydrogels

The temperature-resistance behavior of the nanocomposite hydrogels was investigated as a function of crosslinker amount. As shown in Fig. 5, gel strength of the nanocomposite hydrogels decreased with increasing heating time. With increasing crosslinker amount, the gel strength of the nanocomposite hydrogels decreased more slowly with increasing heating time, demonstrating the enhanced temperature-resistance of the nanocomposite hydrogels. Higher crosslinker amount will cause more crosslink points and higher crosslink density, decreasing the space among the grids of the three-dimensional network, increasing rigidity of the polymeric network, and thus increasing temperature-resistance.

6. Effects of Crosslinker Amount on Swellability of the Nanocomposite Hydrogels

Swellability of the nanocomposite hydrogels synthesized at different crosslinker amount is shown in Fig. 6. As indicated in Fig. 6, the average particle size of the nanocomposite hydrogels synthesized at crosslinker amount of 0.2% and 0.6%, increased from 0.38 μm and 0.12 μm to 4.6 μm and 2.8 μm, respectively, with swelling time increasing from 30 min to 300 min. This indicates the good adjustable swellability of the nanocomposite hydrogels via changing crosslinker amount. With increasing crosslinker amount, denser

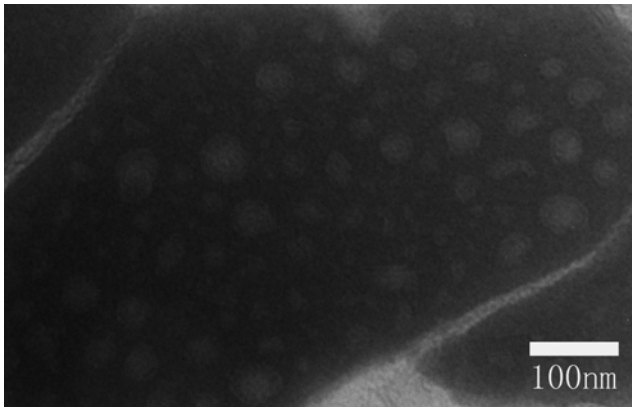

Fig. 7. TEM picture of the as-synthesized nanocomposite hydrogels.

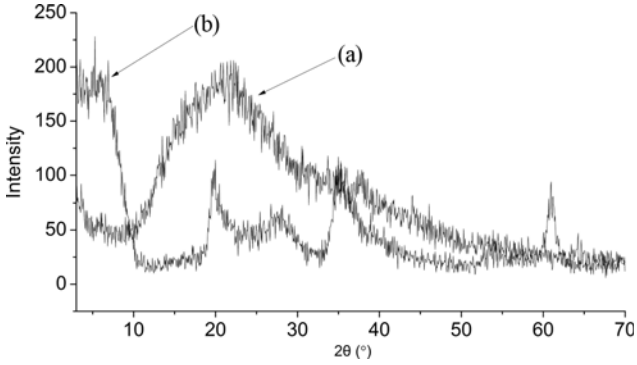

Fig. 8. XRD spectra of the nanocomposite hydrogels (a) and hectorite (b).

and stiffer polymeric networks are formed, preventing the networks from expanding and thus decreasing the swellability of the nanocomposite hydrogels.

7. Morphology and Structure of the Nanocomposite Hydrogels

The morphology and size of the as-synthesized nanocomposite hydrogels were characterized by TEM and the results shown in Fig. 7. Nanocomposite hydrogel particles are regular and spherical-like and have an average particle size of 43 nm in the range of 30-65 nm, indicating that nanocomposite hydrogels have been successfully synthesized by microemulsion polymerization.

8. X-ray Analysis of the Nanocomposite Hydrogels

XRD patterns of hectorite and nanocomposite hydrogels are shown in Fig. 8. As indicated there, hectorite showed five distinct diffraction peaks, an indicative of crystalline structure of hectorite. After graft copolymerizing of hectorite with IA and AM, these diffraction peaks disappeared and were transformed into a large and wide dispersion peak. This confirmed that hectorite clay platelets were exfoliated and transformed into amorphous structure, causing hectorite to be dispersed randomly within the polymeric network.

9. Thermal Analysis (TGA) of the Nanocomposite Hydrogels

TGA and DTGA curves of nanocomposite hydrogels are shown in Fig. 9. As indicated, nanocomposite hydrogels had three step degradations. The first degradation step between 25 and 165 °C with T_{max} of 80 °C, temperature at which maximum degradation occurred, might be due to the water desorption. The second degradation step lying between 175 and 300 °C with T_{max} of 280 °C and onset decomposing temperature (T_{onset}) of 252 °C, is ascribed to the elimination of CO_2 and water molecule from the two neighboring carboxylic groups of the polymer chains due to carboxyl removal and the formation of anhydride [35]. The third degradation step between 300 and 500 °C with T_{max} of 333 °C, is due to the breakage of polymeric chains and the destruction of crosslinked network structure. This clearly indicates the good thermal stability of nanocomposite hydrogels.

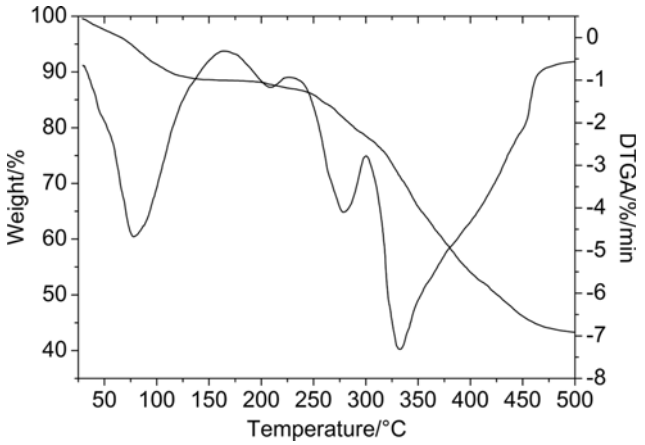

Fig. 9. TGA of the nanocomposite hydrogels.

CONCLUSIONS

A novel hectorite/poly(acrylamide/itaconic acid) nanocomposite hydrogel was synthesized by inverse microemulsion polymerization. With increasing crosslinker amount, water and salt absorbency, pH-sensitivity decreased with the salt absorbency sequence of $Na^+ > Mg^{2+} > Ca^{2+}$, while gel strength and temperature-and shear-resistance increased with gel strength of 13.6 Pa·s at 0.6 wt% crosslinker used. Average particle size of the nanocomposite hydrogels synthesized at 0.2% and 0.6% crosslinker, increased from 0.38 μm and 0.12 μm to 4.6 μm and 2.8 μm, respectively, with swelling time increasing from 30 min to 300 min. TEM indicated that the as-synthesized regular and spherical-like hydrogel particles had an average particle size of 43 nm in the range of 30-65 nm. XRD demonstrated that hectorite clay platelets were exfoliated and transformed into amorphous structure. TGA showed that nanocomposite hydrogels had good thermal stability with onset decomposing temperature of 252 °C.

ACKNOWLEDGEMENT

The authors are grateful for the support of PetroChina Innovation Foundation, China (2012D-5006-0212), Sichuan Provincial Science & Technology Pillar Program, China (2013GZ0149, 2014GZX0010), Opening fund of State Key Laboratory of Geohazard Prevention and Geoenvironment Protection, Chengdu University of Technology, China (SKLGP2012K004) and the Sichuan youth science and technology innovation research team funding scheme, China (2013TD0005).

REFERENCES

1. K. Kosemund, H. Schlatter, J. L. Ochsenhirt, E. L. Krause, D. S. Marsman and G. N. Erasala, *Regul. Toxicol. Pharm*., **53**, 81 (2009).
2. R. Liang, H. B. Yuan, G. X. Xi and Q. X. Zhou, *Carbohyd. Polym*., **77**, 181 (2009).
3. J. C. Duan, Q. Lu, R. W. Chen, Y. Q. Duan, L. F. Wang, L. Gao and S. Y. Pan, *Carbohyd. Polym*., **80**, 436 (2010).
4. M. Sadeghi and H. J. Hosseinzadeh, *J. Bioact. Compat. Polym*., **23**, 381 (2008).
5. P. Tongwa, R. Nygaard and B. J. Bai, *J. Appl. Polym. Sci*., **128**, 787 (2013).
6. J. Hu, T. Kurokawa, T. Nakajima, T. L. Sun, T. Suekama, Z. L. Wu, S. M. Liang and J. P. Gong, *Macromolecules*, **45**, 9445 (2012).
7. S. Hashmi, A. G. Nejad, F. O. Obiweluozor, M. Vatankhah-Varnoosfaderani and F. J. Stadler, *Macromolecules*, **45**, 9804 (2012).
8. K. Okada and A. Usuki, *Macromol. Mater. Eng*., **291**, 1449 (2006).
9. K. Haraguchi and T. Takehisa, *Adv. Mater*., **14**, 1120 (2002).
10. K. Haraguchi, T. Takehisa and S. Fan, *Macromolecules*, **35**, 10162 (2002).
11. K. Haraguchi, R. Farnworth, A. Ohbayashi A and T. Takehisa, *Macromolecules*, **36**, 5732 (2003).
12. M. Fiayyaz, K. M. Zia, M. Zuber, T. Jamil, M. K. Khosa and M. A. Jamal, *Korean J. Chem. Eng*., **31**, 644 (2014).
13. Y. D. Kim and G. G. Hong, *Korean J. Chem. Eng*., **29**, 964 (2012).
14. M. Fukasawa, T. Sakai, U. I. Chung and K. Haraguchi, *Macromolecules*, **43**, 4370 (2010).
15. C. J. Wu and G. Schmidt, *Macromol. Rapid Commun*., **30**, 1492 (2009).
16. C. J. Wu, A. K. Gaharwar, B. K. Chan and G. Schmidt, *Macromolecules*, **44**, 8215 (2011).
17. Y. R. Wang, J. H. Ma, S. G. Yang and J. Xu, *Colloids Surf., A: Physicochem. Eng. Aspects*, **390**, 20 (2011).
18. X. B. Hu, L. J. Xiong, T. Wang, Z. M. Lin, X. X. Liu and Z. Tong, *Polymer*., **50**, 1933 (2009).
19. L. J. Xiong, M. N. Zhu, X. B. Hu, X. X. Liu and Z. Tong, *Macromolecules*, **42**, 3811 (2009).
20. D. Foungfung, S. Phattanarudee, N. Seetapanc and S. Kiatkamjornwong, *Polym. Adv. Technol*., **22**, 635 (2011).
21. M. Kaplan and H. Kasgoz, *Polym. Bull*., **67**, 1153 (2011).
22. T. Wan, L. Xiong, R. Q. Huang, Q. H. Zhao, X. M. Tan, L. L. Qin and J. Y. Hu, *Polym. Bull*., **71**, 371 (2014).
23. T. Wan, R. Q. Huang, Q. H. Zhao, L. Xiong, L. Luo, H. B. Zhang and G. J. Cai, *J. Compos. Mater*., **48**, 2341 (2014).
24. T. Wan, R. Q. Huang, Q. H. Zhao, L. Xiong, L. Luo, X. M. Tan and G. J. Cai, *J. Appl. Polym. Sci*., **130**, 698 (2013).
25. T. Wan, R. Q. Huang, Q. H. Zhao, L. Xiong, L. L. Qin, X. M. Tan and G. J. Cai, *J. Appl. Polym. Sci*., **130**, 3404 (2013).
26. T. Wan, J. Yao, Z. S. Sun, L. Wang and J. Wang, *J. Pet. Sci. Eng*., **78**, 334 (2011).
27. T. Wan, T. S. Zang, Y. C. Wang, R. Zhang and X. C. Sun, *Polym. Bull*., **65**, 565 (2010).
28. T. Wan, C. Wu, X. L. Ma, J. Yao and K. Lu, *Polym. Bull*., **62**, 801 (2009).
29. T. Wan, J. Yao and X. L. Ma, *J. Appl. Polym. Sci*., **110**, 3859 (2008).
30. T. Wan, L. Wang, J. Yao, X. L. Ma, Q. S. Yin and T. S. Zang, *Polym. Bull*., **60**, 431 (2008).
31. T. Wan, X. Q. Wang, Y. Yuan and W. Q. He, *Polym. Int*., **55**, 1413 (2006).
32. T. Wan, X. Q. Wang, Y. Yuan and W. Q. He, *J. Appl. Polym. Sci*., **102**, 2875 (2006).
33. P. J. Flory, *Principles of polymer chemistry*, Ithaca and London: Cornell University Press (1953).
34. P. S. K. Murthy, Y. M. Mohan, J. Sreeramulu and K. M. Raju, *React. Funct. Polym*., **66**, 1482 (2006).
35. Y. H. Huang, J. Lu and C. B. Xiao, *Polym. Degrad. Stab*., **92**, 1072 (2007).